Techno Science Africana Journal **Ibrahim**
Volume 8 Number 1 June, 2013 pp 139 - 147
ISSN 2006 - 2273

TWO-DIMENSIONAL MAGNETIC FIELD MAPPING OF A 3-PHASE INDUCTION MOTOR USING FINITE ELEMENT METHOD

S.B. Ibrahim
Department of Electrical Engineering, Bayero University, Kano

ABSTRACT

Performance characteristics of induction motor are normally evaluated using analytical methods based on approximations to the circuit parameters of the machine to allow for the effect of magnetic saturation. These techniques usually result in inaccuracies in the performance prediction of the motor, as it does not give accurate information on the flux distribution in the motor. A numerical approach was introduced which overcomes these deficiencies through the use of Finite Element Method (FEM) for the prediction of the two-dimensional (2-D) magnetic field mapping of a 3-phase 4-pole, 230V, 50Hz, 1.49A squirrel-cage induction motor. The result obtained from the analyzed FEM model developed for the motor shows the magnetic field pattern of the motor in terms of flux lines and flux density map during the no-load operation of the motor. In addition, the magnetic flux distribution in the air-gap, the variation in electromagnetic torque developed and the variation in the motor phase current during startup are obtained. By examining the obtained flux line and flux density map, the effect of the magnetic field produced by the stator currents at no-load on the rotor is clearly seen, where the magnetic field penetrated the rotor easily due to the high permeability of the rotor. As expected the obtained magnetic flux density distribution in the air-gap of the machine has an envelope waveform that is sinusoidal similar to that of the waveforms of applied stator voltages.
KEYWORDS: Two-dimensional, magnetic field, finite element,mapping, induction motor.

NOMENCLATURE

A = magnetic vector potential
Ω = total cross-sectional area of one phase conductors
ν = reluctivity of the motor's core material
x, y = 2D Cartesian coordinates
σ = conductivity of the material
i = total current in the conductor
u = potential difference induced between the axial ends of a conductor
l = axial length of a conductor
J_m = moment of inertia
ω = rotor speed
T_e = electromagnetic torque
T_f = load torque.
H = magnetic field intensity
J = current density
B = magnetic flux density
μ = core material's absolute permeability.
$\mathbf{A}$ = magnetic vector potential
a, b and c = constants
Δ = area of the *n-th* triangular element
$v_i(x, y)$ = interpolating function
$[A]$, $[i]$ = unknown magnetic vector potentials, current
D, B, $[K]$, $[C]$, $[Q]$ and $[R]$ = coefficient matrices
$[P]$ = vector associated with input voltages
$L_{\sigma 1}$ = stator winding leakage inductance per phase
$L_{\sigma 2}$ = rotor leakage inductance per phase referred to the stator
L_m = mutual inductance

R_{1p} = stator phase winding resistance

R_{2p} = rotor resistance per phase referred to the stator at startup.

T_s = starting torque

T_n = nominal torque

I_p = startup current

I_o = no-load current

S_n = nominal slip

N_n = nominal speed

INTRODUCTION

Usually, electrical machines performance parameters and characteristics are evaluated from formulae based on approximations to actual flux distribution in the machine. Inacurracies in the performance prediction, resulting from these approximations, make it necessary to employ improved analytical models [1-3].

With the advent of modern digital computers, numerical methods have become practical and are being used to improve the accuracy of magnetic field computations in electrical machines. Numerical methods such as Boundary Element Method (BEM), Finite Difference Method (FDM) and Finite Element Method (FEM) are used in computing the magnetic field patterns. Amongst these numerical methods, FEM is the most used method in the prediction of the magnetic field pattern of electrical machines [4], because it can be applied to complex geometrical shape domains, used with homogeneous or heterogeneous materials, boundary conditions can be established relatively easily and the FEM model of the electrical machine is relatively simple when compared with that of other numerical methods [5].

The FEM has been used as a precise dynamic simulation tool for electrical machines [6] for the prediction of performance behavior of the motor, especially at the design stage. The FEM model describes the electromagnetic fields of the machine by finite element equations. The set of equations is then solved directly using FEM solver. Such model takes into account the effect of magnetic saturation, the eddy currents and the rotation of the rotor [7]. The model can be applied in simulating the starting operation of the machine [5, 8-10], predict the magnetic fields and their corresponding steady-state harmonic stray losses [11], as well as assist in analyzing the machine's performance. All these are difficult problems when using traditional analytical methods.

This paper describes the application of FEM for the generation of 2D-magnetic field mapping of a 3-phase induction motor using magnetic vector potential formulation. The method has been applied in the computation of the magnetic vector potential distribution in the air-gap of the motor, the variational electromagnetic torque and phase current in the motor.

The software package, Finite Element Method Magnetics (FEMM Version 4.2) used in this work relieves the user of analytically realizing the geometrical shape domain meshing operations involved in FEM. All that is required of the user is the geometrical drawing of the cross-section of the motor, formulation of the basic governing equations of the induction motor and post processing of results obtained from the output of the FEMM.

The electromagnetic field equation, electric circuit equations and mechanical equations together form the basic equations governing an induction motor [12] and are shown in equations (1) to (3):

$$\frac{\partial}{\partial x}\left[\nu\frac{\partial A}{\partial x}\right]+\frac{\partial}{\partial y}\left[\nu\frac{\partial A}{\partial y}\right]=-J \quad (1)$$

$$i=-\sigma\iint_{\Omega}\left[\frac{\delta A}{\delta t}+\frac{u}{l}\right]d\Omega \quad (2)$$

$$J_m\frac{d\omega}{dt}=T_e-T_f \quad (3)$$

where A is the magnetic vector potential; Ω is the total cross-sectional area of one phase conductors at one side of the machine's coils; ν is the reluctivity of the motor's core material; x and y are the 2D Cartesian coordinates and σ is the conductivity of the material; i is the total current in the conductor; u is the potential difference induced between the axial ends of a conductor; l is the axial length of a conductor; J_m is the moment of inertia; ω is the rotor speed; T_e is the electromagnetic torque and T_f is the load torque.

FORMULATION FOR THE FINITE ELEMENT METHOD

The basic laws of magnetostatic fields are Ampere's law, and the law of conservation of magnetic flux as given by [4] in equations (4), (5) and (6) below:

$\nabla \times H = J$ (Ampere's law) (4)

$\nabla \bullet B = 0$ (Magnetic flux continuity) (5)

$B = \mu H$ (Constitutive relation) (6)

where H is the magnetic field intensity; J is the current density; B is the magnetic flux density and μ is the core material's absolute permeability.

In terms of the magnetic vector potential, $\mathbf{A}$.

$B = \nabla \times \mathbf{A}$ (7)

Applying the vector identity

($\nabla \times \nabla \times F = \nabla(\nabla \bullet F) - \nabla^2 F$) to equations (4) and (6), and substituting $B = \nabla \times \mathbf{A}$, and assuming Coulomb gauge condition ($\nabla \bullet \mathbf{A} = 0$) leads to Poisson's equation for magnetostatic fields:

$$\nabla^2 \mathbf{A} = -\mu J \quad (8)$$

$$\nabla \times \left[\frac{1}{\mu_{(B)}} \nabla \times \mathbf{A} \right] = J \quad (9)$$

In the air-gap of the motor:

$J = 0$ (10)

Thus, equation (8) becomes Laplace's equation given as:

$$\nabla^2 \mathbf{A} = \frac{\partial^2 A}{\partial x^2} + \frac{\partial^2 A}{\partial y^2} = 0 \quad (11)$$

In the rotor conductor domain of the motor, the current density is:

$$J = \frac{-\sigma}{l} u - \sigma \frac{\partial A}{\partial t} \quad (12)$$

and in the stator conductor domain [7]:

$$J = \frac{-\sigma}{l} u - \frac{\sigma \left[\iint_{\Omega} \frac{\partial A}{\partial t} d\Omega - \iint_{\Omega} \frac{\partial A}{\partial t} d\Omega \right]}{\iint_{\Omega} d\Omega} \quad (13)$$

where Ω is the total cross-sectional area of one phase conductors at one side of the machine's coils. The unknown potential difference, u can be eliminated when the circuit equations of the rotor windings and the stator external circuits are introduced [12].

Solution Procedure

Finite element method employs discretization of the solution domain into smaller triangular regions called elements, and the solution to the FEM analysis is determined in terms of discrete values of magnetic vector potential in x, y, z directions at the nodes of the elements.

Considering, 2-D Cartesian coordinate system and triangular elements as shown in Fig. 1, the variation in magnetic vector potentials A_i , A_j and A_k over an element can be defined using the shape Function [13]. The shape is represented by a polynomial approximation of the domain under consideration, consistent with the number of nodes (and associated potential on each edge). The 2D domain is subdivided in a finite and sufficiently high number of elements. The elements in their simplest form are triangles and whose sides are not necessarily equal, but the triangles should not intersect each other as shown in Fig. 1. Each vertex is called a node and all the triangles in a given domain in conjunction with their vertices set up the mesh of the domain.

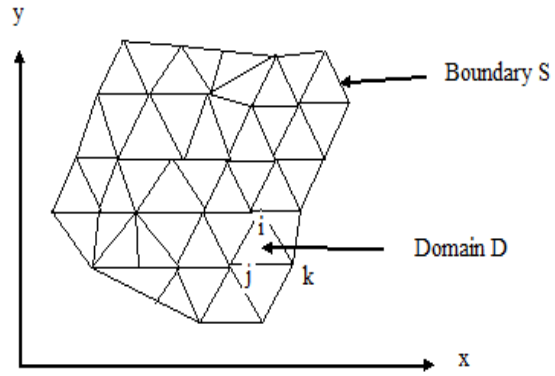

Fig. 1: Discretization of the field region by triangular finite element

Because of the small dimensions of the elements, the interpolating function is simple. In this work, a linear interpolation of the function is assumed for each n-th triangular element, given by

$$A_n(x, y) = a + bx + cy \qquad (14)$$

In particular, in the three nodes of a typical elemental triangle, the three magnetic vector potentials are given by:

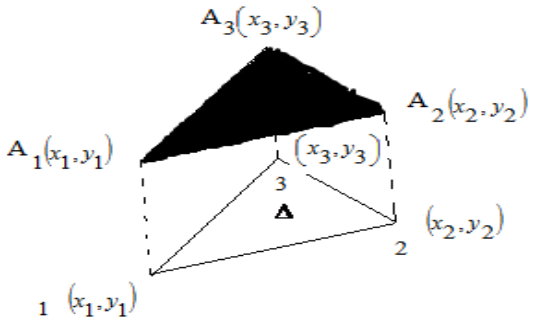

Fig. 2: Linear interpolation of the potential function A_n in the n-th triangular element

$$\begin{aligned} A_i &= A_1 = a + bx_1 + cy_1 \\ A_j &= A_2 = a + bx_2 + cy_2 \\ A_k &= A_3 = a + bx_3 + cy_3 \end{aligned} \qquad (15)$$

where a, b and c are constants to be determined, and x, y are the 2D Cartesian coordinates.
From the knowledge of the value of the function in the nodes of each finite element, i.e., A_1, A_2 and A_3, it is possible to compute the potential function in any other point of the element as represented in Fig. 2. If the three values of the potential are given in the three nodes of the element, it is possible to solve the system equation (15) in the three unknowns a, b and c. Let Δ represents the area of the n-th triangular element, as shown in Fig. 2 and is obtained as:

$$\Delta = \frac{1}{2}\begin{vmatrix} 1 & x_1 & y_1 \\ 1 & x_2 & y_2 \\ 1 & x_3 & y_3 \end{vmatrix} \qquad (16)$$

$$\Delta = \frac{1}{2}\left[\left(x_2 y_3 - x_3 y_2\right) + \left(x_3 y_1 - x_1 y_3\right) + \left(x_1 y_2 - x_2 y_1\right)\right] \quad (17)$$

Using Cramer's rule, the coefficients a, b and c are obtained as:

$$a = \frac{1}{2\Delta}\left[A_1 p_1 + A_2 p_2 + A_3 p_3\right] \quad (18)$$

$$b = \frac{1}{2\Delta}\left[A_1 q_1 + A_2 q_2 + A_3 q_3\right] \quad (19)$$

$$c = \frac{1}{2\Delta}\left[A_1 r_1 + A_2 r_2 + A_3 r_3\right] \quad (20)$$

where

$$p_1 = x_2 y_3 - x_3 y_2 \qquad q_1 = y_2 - y_3 \qquad r_1 = x_3 - x_2$$
$$p_2 = x_3 y_1 - x_1 y_3 \qquad q_2 = y_3 - y_1 \qquad r_2 = x_1 - x_3$$
$$p_3 = x_1 y_2 - x_2 y_1 \qquad q_3 = y_1 - y_2 \qquad r_3 = x_2 - x_1 \quad (21)$$

Equation (14) expresses the unknown magnetic potential function $A_n(x, y)$, inside the *n*-th triangular finite element. It can be written as:

$$A_n(x, y) = \left(\frac{1}{2\Delta}\sum_{i=1}^{3} p_i A_i\right) + \left(\frac{1}{2\Delta}\sum_{i=1}^{3} q_i A_i\right).x + \left(\frac{1}{2\Delta}\sum_{i=1}^{3} r_i A_i\right).y \quad (22)$$

$$A_n(x, y) = \sum_{i=1}^{3} \frac{\left(p_i + q_i x + r_i y\right)}{2\Delta} A_i \quad (23)$$

$$A_n(x, y) = \sum_{i=1}^{3} v_i(x, y) A_i \quad (24)$$

where $v_i(x, y)$ with i=1, 2, 3 is the interpolating function that interpolate the function $A_n(x, y)$.

By finite element discretization of equations (1), (2), (3), (10), (12) and (13), one will subsequently obtain the following large nonlinear system of equations [12]:

$$\begin{bmatrix} K & C \end{bmatrix}\begin{bmatrix} A \\ i \\ \omega \end{bmatrix} + \begin{bmatrix} Q & R \end{bmatrix}\begin{bmatrix} \partial A/\partial t \\ \partial i/\partial t \\ \partial \omega/\partial t \end{bmatrix} = \begin{bmatrix} P \end{bmatrix} \quad (25)$$

where $[A]$, $[i]$, and ω are the unknown magnetic vector potentials, current and rotor speed respectively. $[K]$, $[C]$, $[Q]$ and $[R]$ are coefficient matrices and $[P]$is the vector associated with input voltages. For simplicity, equation (25) can be expressed as:

$$[D][X] + [B]\left[\frac{\partial X}{\partial t}\right] = [P] \quad (26)$$

Where X is an unknown vectors to be evaluated. D and B are coefficient matrices. The system of equations presented in equation (26) is solved using Newton-Raphson method, this is necessary in updating the magnetic permeability of each finite element in terms of magnetic flux density.

Simulation of the FEM Model

FEM allows the simulation of all operating conditions of an induction motor with high accuracy (i.e., the startup operation, no-load operation, nominal loading operation).

The Startup Condition Simulation

To simulate the startup condition of the motor at nominal voltage (230V), the stator winding is supplied by a balanced voltage source.

The rms value of the voltage and frequency are nominal ones and the rotor is locked. The most important at startup condition are the phase current, total leakage inductance and the equivalent rotor resistance of the motor.
The total leakage inductance is determined by magnetic co-energy method, while the equivalent rotor resistance is determined from the Joule loss in the rotor.

No-load Condition Simulation

To simulate no-load condition, the stator winding of the motor is supplied as in the startup condition simulation and with the rotor running at a speed lower than the synchronous speed (corresponding to slip of 0.018). Based on the 2-D time harmonic with motion analysis, the no-load current and magnetization inductance is obtained.

THE ANALYZED MODEL

The FEM model analyzed in this paper represents that of a 3-phase induction motor, with squirrel-cage rotor, the nominal phase voltage is 230V. The stator winding is a single-layer short pitch, with frontal ends in two planes, three slots per pole per phase, 4-pole and 44 turns/slot. The inner stator diameter is 80.75mm, the outer is 130mm, the stator length is 100mm and the air-gap is 0.375mm.
For this motor, the magnetic vector potential distribution in the air-gap when nominal currents of 1.49A flow in the stator winding is shown in Fig. 3

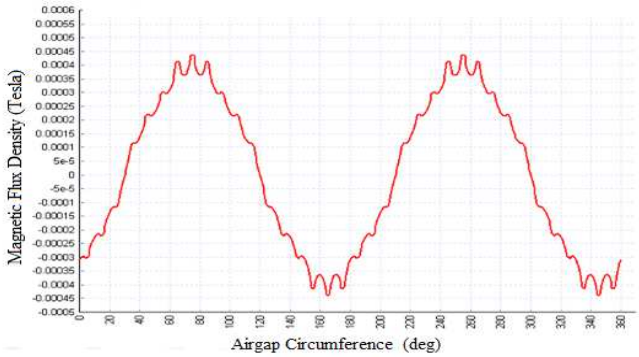

Fig. 3: Magnetic Flux Density Distribution in the Air-gap

One-quarter 2-D numerical model of the motor and its associated generated mesh is presented in Fig. 4.

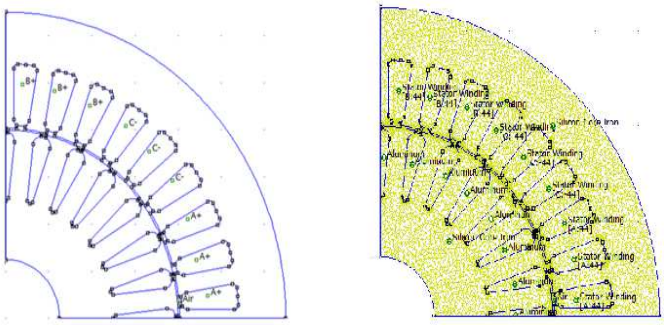

(a) (b)

Fig. 4: 2-D Model (a) One-Quarter of the Motor Geometrical Drawing and (b) Motor's associated generated mesh.

Magnetic field lines and flux density mapping of the cross-section of the motor on no-load condition is shown in Fig. 5.

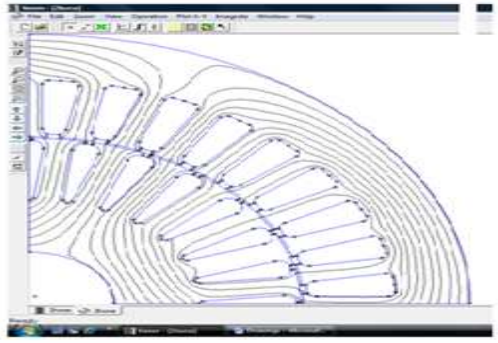

(a)

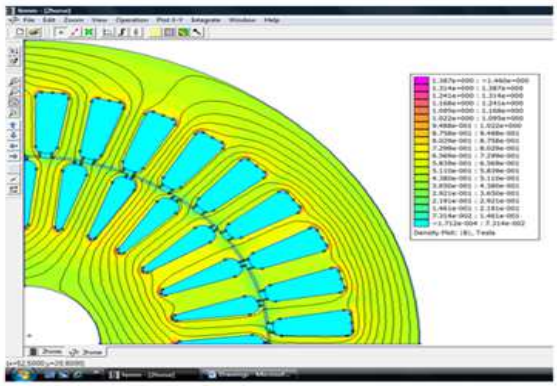

(b)

Fig. 5: (a) Flux Lines and (b) Flux Density Map on No-load Condition

Based on the results obtained from the numerical analysis, the electrical circuit parameters and the operating parameters of the motor have been determined as in Tables 1 and 2:
Table 1: The Electrical Circuit Parameters of the Motor.

Inductances (mH)		**Resistances (Ω)**	
$L_{\sigma 1}$	7.9205	R_{1p}	4.4000
$L_{\sigma 2}$	7.9205	R_{2p}	1.9228
L_m	317.115		

In Table 1, $L_{\sigma 1}$ represents the stator winding leakage inductance per phase, $L_{\sigma 2}$ is the rotor leakage inductance per phase referred to the stator, L_m is the mutual inductance, R_{1p} is the stator phase winding resistance, R_{2p} is the rotor resistance per phase referred to the stator at startup.

Table 2: The Operating Parameters of the Motor.

T_S (Nm)	T_n (Nm)	I_p	I_O	I_p/I_n	S_n	N_n (rpm)
3.12	2.1	2.7	0.29	4.03	0.018	1443

In Table 2, T_S represents the starting torque, T_n is the nominal torque, I_p is the startup current, I_O is the no-load current, S_n is the nominal slip and N_n is the nominal speed. For the motor under consideration a 2-D time harmonic with motion from startup to the synchronous speed analysis has been investigated. The stator phase current variation and the electromagnetic torque variation from startup to the synchronous speed and the magnetization curve of the induction motor are shown in Figs. 6, 7 and 8 respectively.

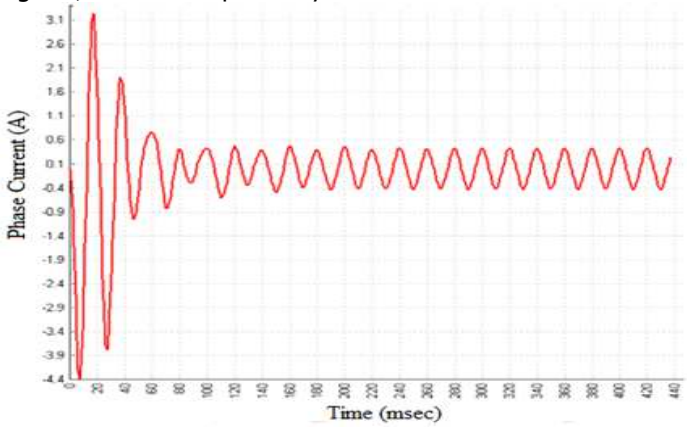

Fig. 6: The Variation of the Phase 'A' Current

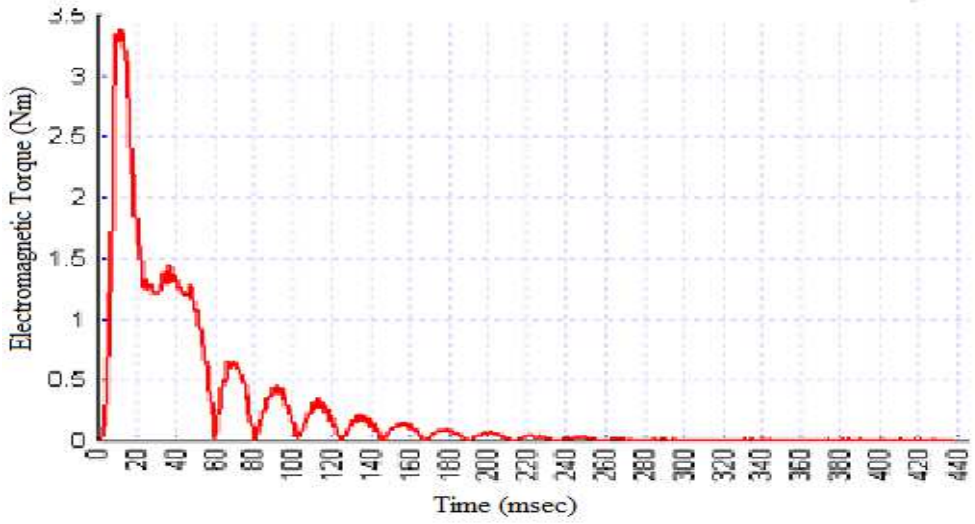

Fig. 7: The Variation of the Electromagnetic Torque

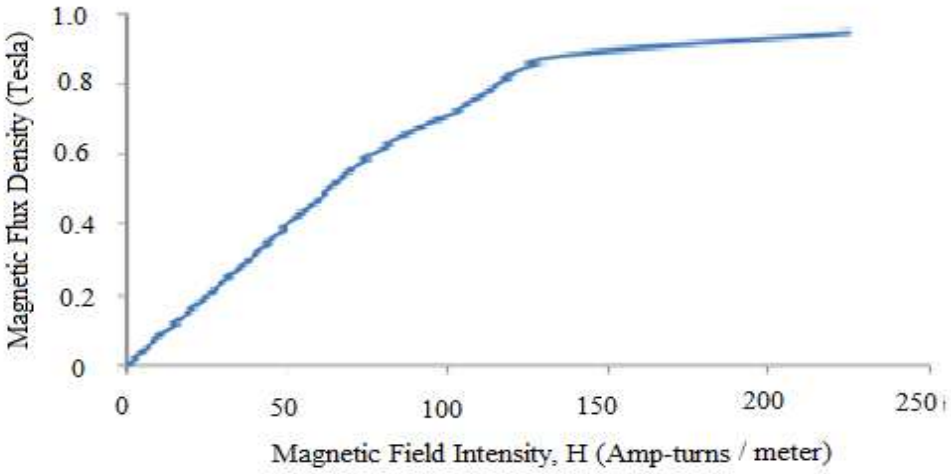

Fig. 8: Magnetization Curve

CONCLUSION

Numerical modeling and analysis using FEM and its application in solving magnetic field problem in a 3-phase induction motor is presented. The formulation and analysis of the FEM model for the induction motor using first-order triangular finite element was discussed. The result of the FEM analysis shows the 2-D magnetic field model of the motor which include the flux lines and flux density map (Fig. 5) of the motor operating on no-load, magnetic flux density distribution in the air-gap of the motor (Fig. 3), the variation in motor's electromagnetic torque Fig. 7), the variation of the motor's phase current (Fig. 6) and the magnetization curve (Fig. 8) of the motor's core material.

It can be observed from the flux lines and flux density map of the motor (Fig. 5) the effect of the magnetic field produced by the currents induced in the rotor circuit of the motor when operating on no-load condition. Under this condition, the values of the currents are at their minimum, and the magnetic field of the stator penetrates easily into the rotor, which is not shielded by the rotor bars current.

Also as expected the variation in the magnetic flux density distribution in the air-gap of the motor has an envelope waveform (Fig. 3) that is sinusoidal similar to that of the waveforms of applied stator voltages.

Among the advantages associated with the analysis using FEM are: it can be applied to complex shape domains, homogeneous or non homogeneous materials, boundary conditions can be established relatively easily and the mathematical model is relatively simple compared to that of the traditional method.

REFERENCES

1. Tandon S.C., Richter E. and Chari M.V.K., "Finite Elements and Electrical Machine Design", IEEE Trans. on Magnetics, Vol. MAG-16, No. 5, Sept., 1980.
2. Pedro J., Bastos A., and Sadowski N., *Electromagnetic Modeling by Finite Elements Method (Electrical and Computer Engineering)*, 1st Edition, Marcel Dekker Inc., New York, Basel, April 2003.
3. Sarac V., "Different Approaches in Numerical Analysis of Electromagnetic Phenomena in Shaded Pole Motor with Application of Finite Elements Method" Proc. of the EMTS Int'l. Symposium of Electromagnetic Theory, pp. 97-100, 2010.
4. Bianchi, N., *Electrical Machine Analysis Using Finite Elements*, 1st Edition, CRC Press, Taylor and Francis Group, USA, 2005.
5. Williamson, S., Lim, L.H. and Smith, A.C., "Transient Analysis of Cage Induction Motors Using Finite Elements", IEEE Trans. MAG-26, Vol.2, pp. 941-944, 1990.
6. Ho, S.L., Fu, W.N., "Status of the Application of Finite Element Method to Induction Machines", Aegean Conference on Electrical Machines and Power Electronics, 5-7 June, 1995.
7. Nandi A. and Neogy S., "An Efficient Scheme for Stability Analysis of Finite Elements Asymmetric Rotor Models in a Rotating Frame", Journal of Finite Elements in Analysis and Design, Vol. 41, No. 14, pp. 1343-1364, Aug 2005.
8. Vassent, E., Meunier, G., et al., "Simulation of Induction Machine Operation Using a step by step Finite Element Method Coupled with Circuits and Mechanical Equations", IEEE Trans. on Magnetics, Vol. 27, No. 6, pp. 5232-5234, Nov. 1991.
9. Philip, G. P and Gregory, K. C., "A Combined Finite Element and Loop Analysis for non-linearity Interacting Magnetic Fields and Circuits", IEEE Trans., Vol. 19, No. 6 pp. 2352-2355, Nov 1983.
10. Min W., Zhang M., Zhu Y. et al "Analysis and Optimization of a New 2-D Magnet Array for Planar Motor", IEEE Trans. on Magnetics, Vol. 6, pp. 153-161, 2010.
11. Ho, S.L., Fu, W.N., "Computation of Harmonic Stray Losses of Induction Motors Using Adaptive Time Stepping Finite Element Method Coupled with Circuits", 7th International Conference on Electrical Machines and Drives, No. 412, pp. 93-97, 11-13 Sept., 1995.
12. Arkkio, A., "Analysis of Induction Motors Based on the Numerical Solution of the Magnetic Field and Circuit Equations", IEEE Trans. MAG-24, Vol. 3, 1987.
13. Reece, A.B.J and Presto, T.W., *Finite Element Methods in Electrical Power Engineering*, Oxford University Press, New York, 2000.